

Functional characterization of nonsynonymous single nucleotide polymorphisms in the electrogenic $\text{Na}^+\text{-HCO}_3^-$ cotransporter NBCe1A

Osamu Yamazaki · Hideomi Yamada · Masashi Suzuki · Shoko Horita · Ayumi Shirai · Motonobu Nakamura · George Seki · Toshiro Fujita

Received: 29 September 2010 / Revised: 10 December 2010 / Accepted: 20 December 2010 / Published online: 14 January 2011
© Springer-Verlag 2011

Abstract The electrogenic $\text{Na}^+\text{-HCO}_3^-$ cotransporter NBCe1 encoded by *SLC4A4* plays essential roles in the regulation of intracellular/extracellular pH. Homozygous mutations in NBCe1 cause proximal renal tubular acidosis associated with ocular abnormalities. In the present study, we tried to perform functional characterization of the four nonsynonymous single nucleotide polymorphisms (SNPs), E122G, S356Y, K558R, and N640I in NBCe1A. Functional analysis in *Xenopus* oocytes revealed that while the K558R variant had a significantly reduced transport activity corresponding to 47% of the wild-type activity, the remaining variants E122G, S356Y, and N640I did not change the NBCe1A activity. Apparent Na^+ affinity of K558R was not different from that of wild-type NBCe1A. Immunohistological analyses in HEK293 cells and MDCK cells indicated that none of these SNPs changed the trafficking behaviors of NBCe1A. Functional analysis in HEK293 cells also revealed that only the K558R variant had a reduced transport activity, corresponding to 41–47% of the wild-type activity. From these results, we conclude that among four SNPs, only the K558R variant, which is predicted to lie in transmembrane segment 5, significantly reduces the NBCe1A activity without changing the trafficking behavior or the apparent extracellular Na^+ affinity.

Keywords pRTA · SLC4A4 · SNP · Renal proximal tubules

Introduction

The regulation of extracellular and intracellular pH within the optimal ranges is essential for a variety of cellular functions. This task is accomplished by several acid/base transporters. Among them, the electrogenic $\text{Na}^+\text{-HCO}_3^-$ cotransporter NBCe1 encoded by *SLC4A4* has three splice variants that mediate different physiological roles [1, 7, 34]. The kidney-type cotransporter NBCe1A, predominantly expressed in the basolateral membrane of renal proximal tubules, mediates a majority of bicarbonate exit from renal proximal tubules, thereby performing an essential role in the systemic acid/base balance [3, 33, 34]. On the other hand, the pancreas-type cotransporter NBCe1B, in which the first 41 amino acids of NBCe1A are replaced by the unique 85 amino acids, is widely expressed in different types of tissues including pancreatic ducts [20, 21, 32, 35, 36], intestinal tracts [5, 22], corneal endothelium and lens epithelium [8, 42], and astrocytes [9, 11]. Bicarbonate uptake into cells through NBCe1B is thought to be essential for the biological processes such as the maintenance of homeostasis in cornea and lens [8, 42], the pancreatic bicarbonate secretion [20, 36], and the regulation of local pH in the brain [11, 37]. The brain-type cotransporter NBCe1C, the C-terminal variant skipping exon 24, is mainly expressed in brain, but its physiological role remains to be established [7].

Homozygous inactivating mutations in NBCe1 cause proximal renal tubule acidosis (pRTA) associated with ocular abnormalities such as bandkeratopathy, cataract, and glaucoma. So far, 12 homozygous NBCe1A mutations have been reported. They are eight missense mutations (R298S, S427L, T485S, G486R, R510H, L522P, A799V, and R881C) [13, 14, 16, 17, 39], two nonsense mutations

O. Yamazaki · H. Yamada · M. Suzuki · S. Horita · A. Shirai · M. Nakamura · G. Seki (✉) · T. Fujita
Department of Internal Medicine, Faculty of Medicine,
University of Tokyo,
7-3-1 Bunkyo-ku, Hongo,
Tokyo 113-0033, Japan
e-mail: georgeseki-tky@umin.ac.jp

(Q29X and W516X) [18, 30], and two frameshift mutations (2311 delA, S982NfsX4) [19, 40]. Functional analysis using different expression systems suggested that at least 50% reduction in the transport activity of NBCe1A would be necessary to induce the severe pRTA, defined as the reduction of blood HCO_3^- concentration to less than 13 mM [16, 39]. The close inspection of individual pRTA cases, however, revealed no tight relationship between the degree of NBCe1A inactivation and the severity of pRTA, suggesting that factor(s) other than the inactivation of transport function per se would be also involved. Indeed, several missense mutations such R298S, S427L, R510H, L522P, and R881C showed trafficking defects in the polarized Madin–Darby canine kidney (MDCK) cells [28, 39, 41]. Moreover, the NBCe1B mutants, corresponding to R510H, L522P, R881C, and S982NfsX4 mutations in NBCe1A, showed almost no transport activities due to defective membrane expression in human embryonic kidney (HEK293) cells, which seems to be linked to the occurrence of migraine through the near total inactivation of NBCe1 activity in astrocytes [40]. In addition to these naturally occurring mutations linked to pRTA and extrarenal manifestations, an extensive mutagenesis study revealed several amino acid residues of NBCe1 critical for the normal transport functions [2]. Furthermore, a C-terminal motif essential for the proper NBCe1 trafficking was also identified [27]. However, the detailed structural basis of NBCe1-mediated $\text{Na}^+-\text{HCO}_3^-$ cotransport across the plasma membrane is still largely unknown.

Besides its fundamental role as a major bicarbonate exit pathway, NBCe1A may also play an important role in the net sodium reabsorption process in renal proximal tubules. Approximately 60% of the NaCl filtered from glomerulus is reabsorbed in proximal tubules, and this process is facilitated by the coordinated operation of the apical Na^+/H^+ exchanger isoform 3 (NHE3) and the basolateral NBCe1A, with accompanying water absorption [43]. Notably, NHE3-deficient mice show hypotension, even after the transgenic rescue of intestinal absorptive defect [44]. Therefore, functional alterations in NBCe1A can be also theoretically linked to blood pressure variations. Indeed, NBCe1A in proximal tubules is one of target transporters that are stimulated by angiotensin II, a hormone implicated in blood pressure control at least partially by stimulating sodium reabsorption from proximal tubules [12, 29]. Moreover, spontaneously hypertension rats show the defective inhibition of NBCe1A activity by dopamine [26]. In the present study, we attempted to perform functional characterization of nonsynonymous single nucleotide polymorphisms (SNPs) in NBCe1A. Among four nonsynonymous SNPs that have been reported (<http://www.ncbi.nlm.nih.gov/snp/>), we revealed that only the

K558R variant inactivates the transport function without impairing the trafficking behavior or the extracellular Na^+ affinity.

Methods

Construction of NBCe1A expressing constructs

cDNAs encoding human NBCe1A was subcloned into pcDNA3.1 as described [16, 39]. The QuikChange Site-Directed Mutagenesis kit (Stratagene) was used to introduce mutations. Sense primers used to introduce mutagenesis were 5'-GAGCTGAGGACATGTATGGGGAAAGGATC CATCATGCTTG-3' (for E122G), 5'-CTAAGAGTCTTC CATCCTATGACAAAAGAAAGAATATG-3' (for S356Y), 5'-CTTTATCTATGATGCTTTCAAGAGGATGAT CAAGCTTGCAGATTAC-3' (for K558R), and 5'-GGAG GAAACCTCGTCGGGATCAACTGTAATTTTGTTCCTG-3' (for N640I). For GFP-tagged constructs, coding sequences of NBCe1A were subcloned into pcDNA3.1/NH2-terminal GFP-TOPO (Invitrogen). The complete cDNA sequence of each construct was verified by DNA sequencing.

Oocytes preparation

cRNAs were transcribed from the appropriately linearized templates with the mMACHINE high-yield Capped RNA Transcription kit (Ambion). Oocytes were removed from *Xenopus laevis*, dissociated with collagenase as described [16, 39], and were injected with 50 nl of cRNA solution containing 5 ng of cRNA expressing each NBCe1A construct. Electrophysiological studies were performed 3–5 days after cRNA injection. To determine the electrophysiological activities of NBCe1A, we analyzed at least three different batches of oocytes, and the wild-type and SNP variants were analyzed on the same days.

Electrophysiological analysis

Nominally HCO_3^- -free ND96 solution contained (in mM) 96 NaCl, 2 KCl, 1 MgCl_2 , 1.8 CaCl_2 , and 5 mM HEPES at a pH of 7.4. HCO_3^- -containing solution was prepared by replacing 30 mM NaCl with 30 mM NaHCO_3 in ND96, and was equilibrated with 5% CO_2 in oxygen (pH 7.4). Electrophysiological studies were performed as described [16, 39]. In brief, an oocyte was placed in a perfusion chamber and superfused with ND96 solution at a rate of ~4 ml/min. To measure the NBCe1A-mediated current, a two-electrode voltage clamp method was used with a model CEZ-1200 dual-electrode voltage clamp amplifier (NIHON KOHDEN) connected to a Duo773 high input impedance differential electrometer (WPI), controlled by the Clampex

module of pCLAMP software (Axon Instruments). We monitored the NBCe1A currents induced by solution changes from ND96 to HCO_3^- -containing solution at a holding potential of -25 mV, because the baseline current was minimal at this voltage when oocytes were bathed in ND96 solution [16, 39]. In oocytes injected with H_2O , solution changes from ND96 to HCO_3^- -containing solution did not induce any currents as described [16, 19, 39].

To determine the apparent Na^+ affinity of NBCe1A, extracellular Na^+ concentrations were sequentially reduced from 96 to 48, 24, 12, and 0 mM, while the NBCe1A currents were continuously monitored at a holding potential of -25 mV as reported [16]. The current at 0 mM Na^+ was subtracted from the raw data to obtain the corrected currents at the individual Na^+ concentrations. Damping Gauss–Newton method was used to fit data into the Michaelis–Menten equation as described [16].

Expression in cultured cells

MDCK and HEK293 cells were grown on culture dishes in Dulbecco's modified Eagles's medium supplemented with 10% fetal calf serum. These cells were transfected with plasmid expressing each NBCe1A construct with LipofectAMINE 2000 (Invitrogen). The same amounts of DNA (4 μg per well of 6-well dishes or 24 μg per dish of 10-cm dishes) were transfected for the wild-type NBCe1A and the mutants. The cell pH measurement, immunoblotting, or immunofluorescence analyses were performed 48 h after transfection.

Cell pH measurements

HEPES-buffered solution contained (in mM) 127 NaCl, 5 KCl, 1.5 CaCl_2 , 1 MgCl_2 , 2 NaH_2PO_4 , 1 Na_2SO_4 , 25 HEPES, 5.5 glucose; adjusted to pH 7.4 by 1 N NaOH. HCO_3^- -Ringer solution contained (in mM) 115 NaCl, 5 KCl, 1.5 CaCl_2 , 1 MgCl_2 , 2 NaH_2PO_4 , 1 Na_2SO_4 , 25 NaHCO_3 , 5.5 glucose; pH 7.4 equilibrated with 5% CO_2 /95% O_2 gas. Na^+ was replaced by N-methyl-D-glucamine in Na^+ -free HCO_3^- solution and Na^+ -free HEPES solution. HEK293 cells were grown on fibronectin-coated coverslips. Two days after transfection, cells were incubated with the pH dye acetoxymethylester of bis(carboxyethyl)carboxyfluorescein (BCECF/AM; Molecular Probes). Cell pH measurements were performed with a microscopic fluorescence photometry system (OSP-10; Olympus) as described [40]. The intracellular dye was alternatively excited at two wavelengths (440 and 490 nm), and emission was measured at a wavelength of 530 nm. NBCe1A activity in HEK293 cells was analyzed by monitoring Na^+ - and HCO_3^- -dependent cell pH recovery as described [40]. In brief, cells were first superfused with HEPES-buffered Ringer

solution. Solution was exchanged to Na^+ -free HCO_3^- solution, which induced a marked intracellular acidification due to CO_2 entry. Thereafter, solution was exchanged to HCO_3^- -Ringer solution containing 1 mM amiloride, which blocks the endogenous Na^+/H^+ exchange activity. The resultant Na^+ - and HCO_3^- -dependent cell pH recovery (dpH_i/dt) represents the NBCe1A activity [40]. In some experiments, cell pH recovery was induced by HCO_3^- -Ringer solution containing both 1 mM amiloride and 0.5 mM 4, 4'-diisothiocyanatostilbene-2, 2'-disulphonic acid (DIDS, Sigma). To examine the NBCe1A activity in the absence of $\text{HCO}_3^-/\text{CO}_2$, cell pH measurements were performed in HEPES-buffered solutions. In this case, cells were first superfused with HEPES-buffered Ringer solution. To induce an intracellular acidification, cells were superfused for 1–2 min with NH_4Cl -containing solution, which replaces 20 mM NaCl in HEPES-buffered Ringer solution with the equimolar amount of NH_4Cl . After cells were superfused with Na^+ -free HEPES solution, solution was finally exchanged to HEPES-buffered Ringer solution containing 1 mM amiloride. These HEPES-buffered solutions were bubbled with 100% O_2 gas. The intrinsic cell buffer capacity (β_i) was measured with the NH_4Cl pulse method as described [16]. The relationship between cell pH and β_i was shown in Fig. 1. Total cell buffer capacity (β_T) in the HCO_3^- -containing solution was equal to the sum of β_i and the HCO_3^- buffer capacity ($\beta_{\text{HCO}_3^-}$), and the HCO_3^- flux through NBCe1A was calculated as $\text{dpH}_i/\text{dt} \times \beta_T$. The calibration curve for cell pH was made as described [39]. In brief, cells were exposed to HEPES-buffered solution containing 120 mM K^+ and 10 μM nigericin. Solution pH was adjusted at the different levels (from 6.4 to 7.6) with 1 N NaOH, whereas Na^+ concentration in solution was kept constant at 20 mM.

Cell surface biotinylation

Cell surface biotinylation in HEK293 cells was performed with the Pierce Cell Surface Protein Isolation Kit (Thermo

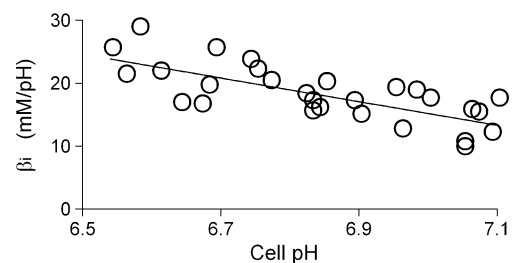


Fig. 1 The relationship between cell pH and β_i in HEK293 cells transfected with vector. The NH_4Cl pulse method was used, and β_i measured at cell pH of 6.7–6.9 was 18.5 ± 0.9 mM/pH ($n=10$). The line represents the linear regression, where the coefficient of determination (R^2) is 0.54

Scientific) according to the manufacturer's protocol. In brief, cells, grown on four dishes of 10-cm culture dish, were washed with phosphate-buffered saline (PBS), incubated with EZ-LINK Sulfo-NHS-SS-biotin for 30 min at 4°C followed by the addition of a quenching solution. Cells were lysed with lysis buffer (500 µl) containing the Halt protease inhibitor cocktail kit. An aliquot (100 µl) of the lysate (total) was saved for Western blotting. The biotinylated NBCe1A was isolated with NeutrAvidin agarose gel, eluted by the sample buffer (400 µl) containing dithiothreitol, and subjected for immunoblotting as described [39]. In brief, after being dissolved in a sample-loading buffer that contained 2% SDS, the protein samples were separated by sodium dodecyl sulfate polyacrylamide gel electrophoresis on acrylamide minigels and transferred to a nitrocellulose membrane. After incubation in a blocking buffer, the membrane was treated with a diluted rabbit polyclonal anti-GFP antibody (Invitrogen) or a rabbit polyclonal anti-Na/K pump $\alpha 1$ antibody (Upstate Biotech) as described [40]. Thereafter, horseradish peroxidase-conjugated anti-rabbit IgG (BioRad) were used as the secondary antibody. The signal was detected by an ECL Plus system (Amersham).

Immunofluorescence

HEK293 cells or confluent MDCK cells were grown on fibronectin-coated coverslips. The confluent MDCK cells on coverslips were shown to retain the proper cell polarity, as evidenced by the basolateral distribution of Na/K pump and the formation of tight junctions [39, 41]. Moreover, the expression of NBCe1 was shown to be more efficient in this condition than when they were grown on permeable supports [41]. The cells were fixed in 4% paraformaldehyde in PBS, permeabilized with 0.1% Triton X-100 (Sigma) in PBS, stained with the F-actin dye tetramethylrhodamine isothiocyanate-phalloidin (Sigma), and observed by a TCS SL laser-scanning confocal microscope (Leica) as described [39, 40]. To visualize the GFP-untagged NBCe1A constructs in MDCK cells, a rabbit polyclonal antibody against C-terminal region (amino acids 928–1035) of NBCe1 (Chemicon) was used as the primary antibody, and Alexa Fluor 488 goat anti-rabbit IgG (Molecular Probes) was used as the secondary antibody as described [39]. We performed at least three independent transfection studies examining at least 100 NBCe1A expressing cells in each case.

Statistical analysis

The data were represented as mean \pm SEM. Significant differences were determined by applying Student's *t* test or ANOVA with Bonferroni's correction, as appropriate. Statistical significance was set at $p < 0.05$.

Results

Functional analysis in *Xenopus* oocytes

Four nonsynonymous SNPs (E122G, S356Y, K558R, and N640I) within the SLC4A4 gene encoding variant NBCe1A transporters have been reported (<http://www.ncbi.nlm.nih.gov/snp/>) as shown in Fig. 2. Allele frequency is reported only for the K558R variant (0.014 in pilot.1. CEU population assembled by 1000 Genomes Project) and the N640I variant (0.013 in AGI_ASP population consisting of Caucasian and African-American females). The clinical phenotypes of carriers for these variants were not reported. To examine the effects of SNPs on NBCe1A function, we first performed the electrophysiological analysis in *Xenopus* oocytes using the GFP-untagged constructs, which have been used to characterize the electrogenic properties of NBCe1 [16, 19, 38, 39]. We monitored the outward currents induced by the solution exchange from ND96 solution to HCO₃⁻-containing solution at a holding potential of -25 mV, which reliably reflect the NBCe1A currents [16, 19, 38, 39]. As shown in Fig. 3a, the E122G, S356Y, and N640I variants had electrogenic activities comparable to that of wild-type NBCe1A. However, the K558R variant had a reduced activity ($p < 0.01$) corresponding to 47.0 \pm 5.4% of that of wild-type NBCe1A.

Apparent Na⁺ affinity

To clarify the effects of K558R variant on NBCe1A properties in more detail, we examined the apparent Na⁺ affinity as described [16]. The current was continuously

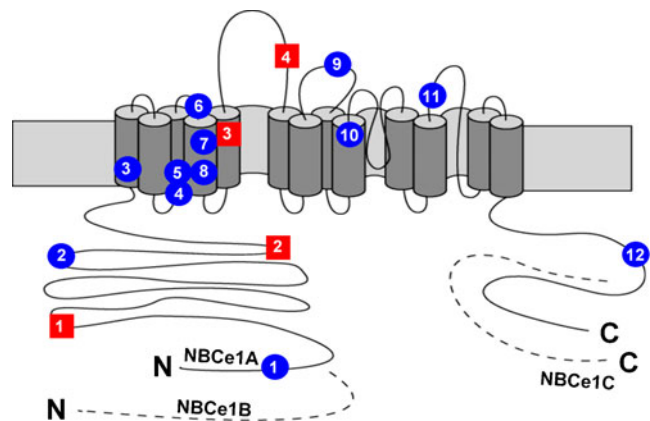


Fig. 2 Topological model of NBCe1A according to the model for AE1 [31]. Red squares show the localization of SNP variants E122G (1), S356Y (2), K558R (3), and N640I (4). Blue circles show the localization of pRTA-related mutations Q29X (1), R298S (2), S427L (3), T485S (4), G486R (5), R510H (6), W516X (7), L522P (8), 2311 delA (9), A799V (10), R881C (11), and S982NfsX4 (12). The dashed lines represent the specific regions of NBCe1B or NBCe1C, and the N and C denote the N- and C-terminus, respectively

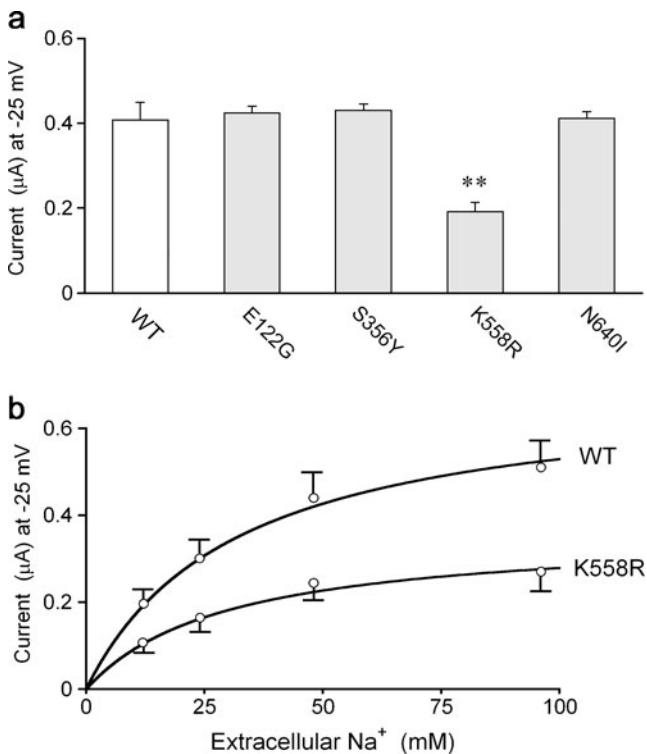


Fig. 3 Functional analysis of SNP variants in *Xenopus* oocytes. **a** Summary of NBCe1 currents elicited by solution change from ND96 to HCO₃⁻ containing solution; ** $p < 0.01$ vs. wild-type (WT). Numbers of observations are 19 (WT), 10 (E122G), 10 (S356Y), 16 (K558R), and 10 (N640I). **b** Apparent Na⁺ affinity for WT and K558R, determined by current monitoring during sequential reduction of extracellular Na⁺ concentrations. Damping Gauss–Newton method was used to fit data into the Michaelis–Menten equation. Numbers of observation are six for WT and seven for K558R

monitored at a holding potential of -25 mV, whereas extracellular Na⁺ concentrations were changed sequentially from 96 mM to 48, 24, 12, and 0 mM. By subtracting the current at 0 mM Na⁺ from raw data and fitting these data into the Michaelis–Menten equation through nonlinear regression analysis, we obtained an individual curve for the wild-type and the K558R variant as shown in Fig. 3b. The calculated Km values of wild-type (31.7 ± 3.9 mM, $n=6$) and K558R (29.6 ± 0.8 mM, $n=7$) were not statically different, indicating that the reduced activity of K558R variant is not due to the reduction in apparent extracellular Na⁺ affinity.

Intracellular expression in mammalian cells

Theoretically, NBCe1A mutations can reduce the overall transport function through the inactivation of individual transporter and/or the reduction in membrane expression. Furthermore, the previous studies suggested that the *Xenopus* oocytes expression system may not be ideal for the detection of trafficking abnormalities of NBCe1

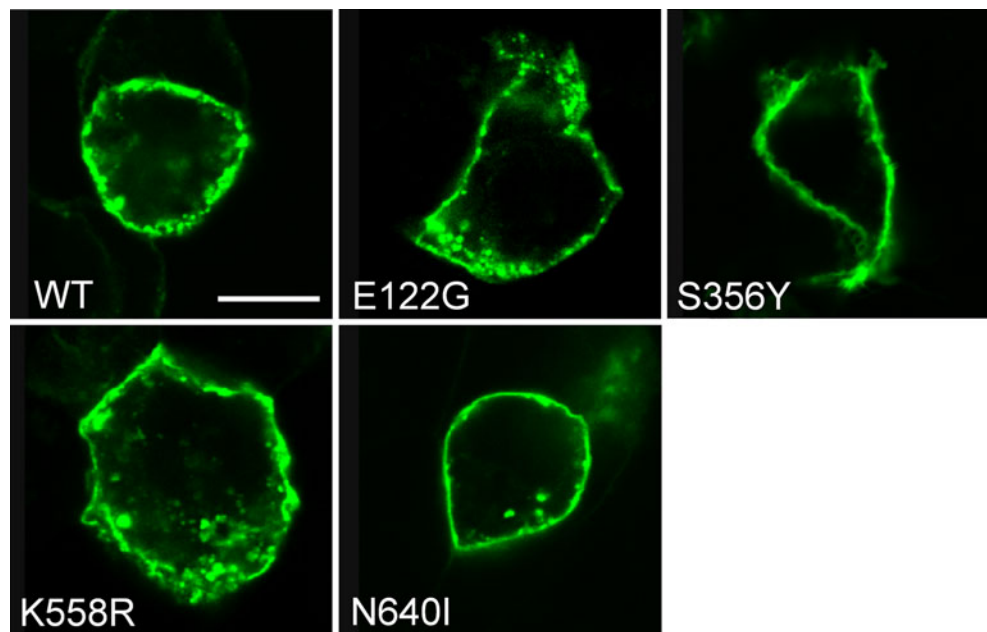
mutants [16, 39, 40]. Therefore, we performed the confocal microscopic analysis to examine the intracellular expression of wild-type and the variants in mammalian cells using the GFP-tagged constructs.

In non-polarized HEK293 cells, the E122G, S356Y, K558R, and N640I variants showed the distinct membrane expression, which was very similar to that of wild-type NBCe1A (Fig. 4). These results indicate that these NBCe1A variants do not show abnormal trafficking in the non-polarized cells. On the other hand, the pRTA-related mutant R298S was reported to show the abnormal trafficking only in the polarized epithelium [16, 28, 39]. Accordingly, we also examined the intracellular expression in confluent MDCK cells, which have been thought to be useful for the analysis of NBCe1 trafficking in the polarized cells [28, 39–41]. As shown in Fig. 5a, the wild-type NBCe1A showed the predominant basolateral membrane expression as reported [39]. As shown in Fig. 5b, the E122G, S356Y, K558R, and N640I variants also showed the predominant basolateral membrane expression, which was indistinguishable from that of wild-type NBCe1A. To exclude any potential influence of the addition of GFP tag, we also examined the intracellular expression of GFP-untagged constructs using the anti-NBCe1 antibody. As shown in Fig. 5c, all these constructs showed the predominant basolateral expression. These results indicate that none of SNPs variants show abnormal trafficking in the polarized mammalian cells.

Functional analysis in HEK293 cells

We next performed the functional analysis in HEK293 cells, which have been widely used to examine the transport function of NBCe1 [4, 24, 40, 45]. We used the GFP-tagged constructs, which have been shown to be useful in this system [6]. Solution exchange from HEPES-buffered solution to Na⁺-free HCO₃⁻ solution rapidly reduced intracellular pH to around 6.8. As shown in Fig. 6a, cells transfected vector alone did not show cell pH recovery upon Na⁺ addition as previously reported [40]. On the other hand, cells transfected with wild-type NBCe1A showed a prompt cell pH recovery upon Na⁺ addition, and this cell pH recovery was completely inhibited by 0.5 mM DIDS as shown in Fig. 6b. The rates of cell pH recovery of wild-type were 0.67 ± 0.05 pH/min in the absence ($n=26$) and -0.03 ± 0.02 pH/min ($n=6$) in the presence of DIDS ($p < 0.01$), respectively. Cells transfected with the K558R variant also showed a prompt cell pH recovery upon Na⁺-addition, but the rate of Na⁺-dependent cell pH recovery was less than that of wild-type as shown in Fig. 6c. Consistent with the previous report [2], β_i (18.5 mM/pH) measured at the intracellular pH of 6.7–6.9 in HEK293 cells transfected by vector alone was unaffected

Fig. 4 Intracellular localization of wild-type (WT) and SNP variants in HEK293 cells. GFP-tagged NBCe1A constructs are shown in *green*. Only front views are shown. Note the predominant membrane expression of WT and SNPs. Bar 10 μm



by transfection with the wild-type NBCe1A or the SNP variants. The initial cell pH values at which cells started Na^+ -dependent pH recovery were used to calculate $\beta_{\text{HCO}_3^-}$. With these β_i and $\beta_{\text{HCO}_3^-}$ values, we obtained β_T values to calculate the HCO_3^- flux mediated by NBCe1A. As summarized in Fig. 6d, the E122G, S356Y, and N640I variants had transport activities comparable to that of wild-type. However, the K558R variant had a reduced transport activity ($p < 0.01$) corresponding to $40.8 \pm 2.7\%$ of that of wild-type NBCe1A. To exclude any potential influence of the addition of GFP tag, we also performed functional analysis in HEK293 cells using the GFP-untagged constructs. As shown in Fig. 6e, we obtained the essentially similar results: only the K558R variant had a significantly reduced activity ($p < 0.05$) corresponding to $46.7 \pm 5.5\%$ of that of wild-type NBCe1A.

The confocal microscopic analysis in HEK293 cells confirmed that the transfection efficiency of the GFP-tagged constructs (60–80%) was similar among wild-type and the SNP variants. To quantify the membrane expression levels of GFP-tagged wild-type and the variants, we performed the cell surface biotinylation Western blotting. As shown in Fig. 7, all the variants showed the similar membrane expression as the wild-type NBCe1A. They also showed the similar whole cell expression as the wild-type NBCe1. These results indicate that only the K558R variant has a reduced transport activity, and that this reduction is not associated with any trafficking abnormalities.

In a separate set of experiments performed with HEPES-buffered solutions, we finally examined the HCO_3^- dependency of NBCe1A activity in HEK293 cells. As shown in Fig. 8, GFP-tagged wild-type NBCe1A showed a slow cell pH recovery even in the absence of $\text{HCO}_3^-/\text{CO}_2$.

The rates of cell pH recovery were 0.13 ± 0.02 pH/min for wild-type ($n=10$) and 0.02 ± 0.01 pH/min ($n=8$) for vector ($p < 0.01$), respectively. We confirmed that 0.5 mM DIDS completely inhibited the slow cell pH recovery by wild-type ($n=5$). The NBCe1A-mediated base flux in the absence of $\text{HCO}_3^-/\text{CO}_2$ calculated by the β_i value (18.5 mM/pH) and the rate of cell pH recovery (0.13 pH/min) was 2.4 ± 0.2 mM/min ($n=10$). This value corresponded to only 11.1% of the NBCe1A-mediated HCO_3^- flux (21.7 ± 1.7 mM/min, $n=26$) calculated by the β_T value (32.6 mM/pH) and the rate of cell pH recovery (0.67 pH/min) in the presence of $\text{HCO}_3^-/\text{CO}_2$. The absolute dependence on Na^+ , the inhibition by DIDS, and the very low affinity to OH^- , if any, shown in this study were consistent with the properties of NBCe1A activity in HEK293 cells [4].

Discussion

In the present study, we tried to perform functional characterization of the four nonsynonymous SNPs, E122G, S356Y, K558R, and N640I in NBCe1A. Because NBCe1 mutations are known to display variable trafficking behaviors depending on the expression systems [16, 28, 39, 41], we used several different approaches to clarify the effects of SNP variants. According to the topology models [31, 45], NBCe1 is presumed to have 13 or 14 transmembrane segments (TMs). Both models predict the E122G and S356Y variants in the N-terminal cytoplasmic region, the K558R variant in near the extracellular end of TM5, and the N640I variant in the extracellular loop between TM5 and TM6. Functional analysis in *Xenopus* oocytes revealed

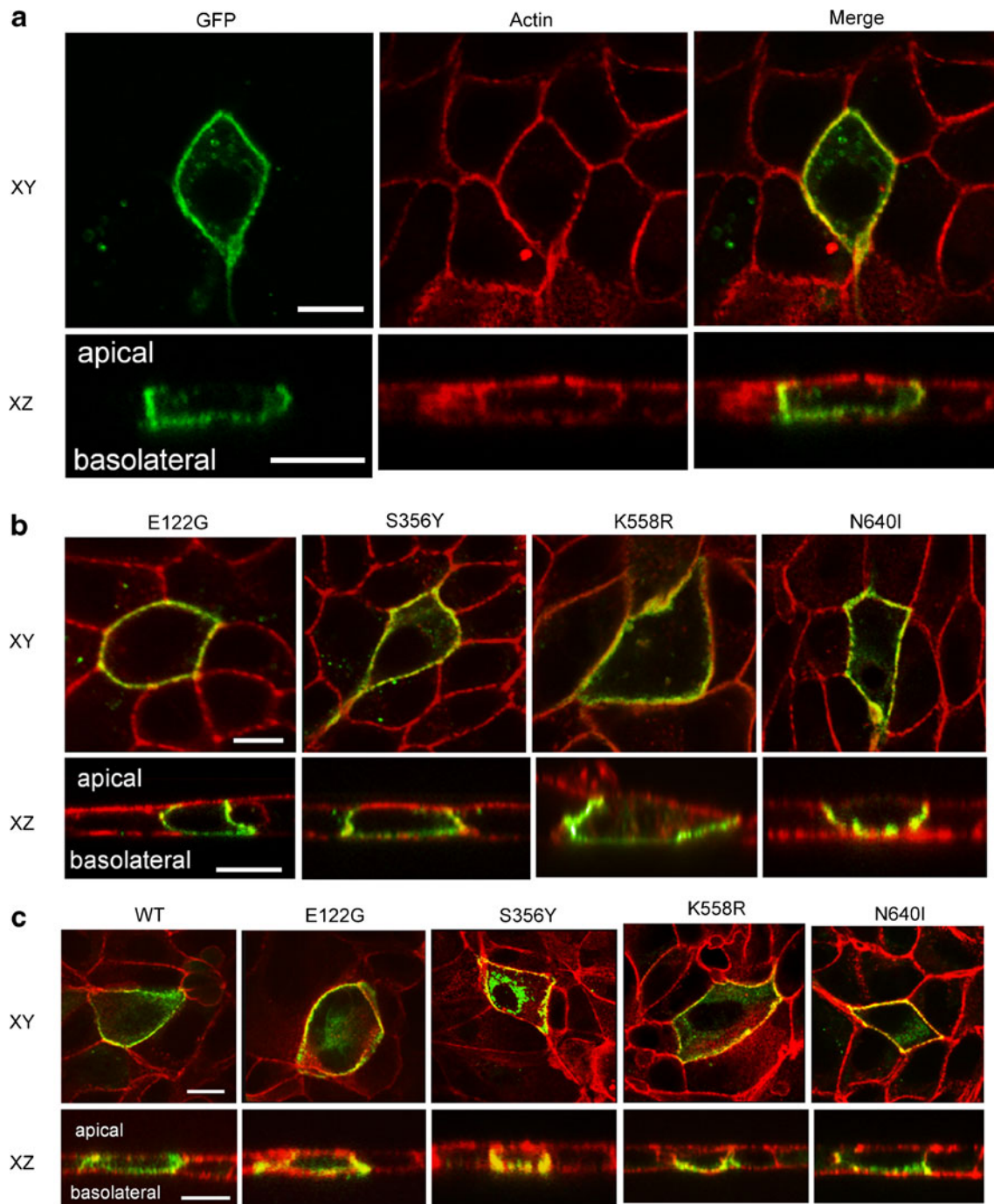


Fig. 5 Intracellular localization in MDCK cells. **a** Expression of GFP-tagged wild-type NBCe1A (*WT*) is shown in *green* and actin as *red*. *XY* indicates front view, and *XZ* side view. Note the predominant basolateral expression of NBCe1A. Bars 10 μm . **b** Expression of

GFP-tagged SNP variants. Note the similar basolateral expression of SNP variants. Details as in Fig. 5a. **c** Expression of GFP untagged constructs detected by the anti-NBCe1 antibody. Details as in Fig. 5a

that while the K558R variant had a significantly reduced transport activity corresponding to 47% of the wild-type activity, the remaining variants E122G, S356Y, and N640I did not change the NBCe1A activity. Apparent Na^+ affinity of K558R was not different from that of wild-type, indicating that the functional reduction of K558R variant

is not due to the reduction in Na^+ affinity. Immunohistochemical analyses in HEK293 cells and MDCK cells indicated that none of these SNPs changed the trafficking behaviors of NBCe1A. Functional analysis in HEK293 cells also revealed that only the K558R variant had a reduced transport activity, corresponding to 41–47% of the

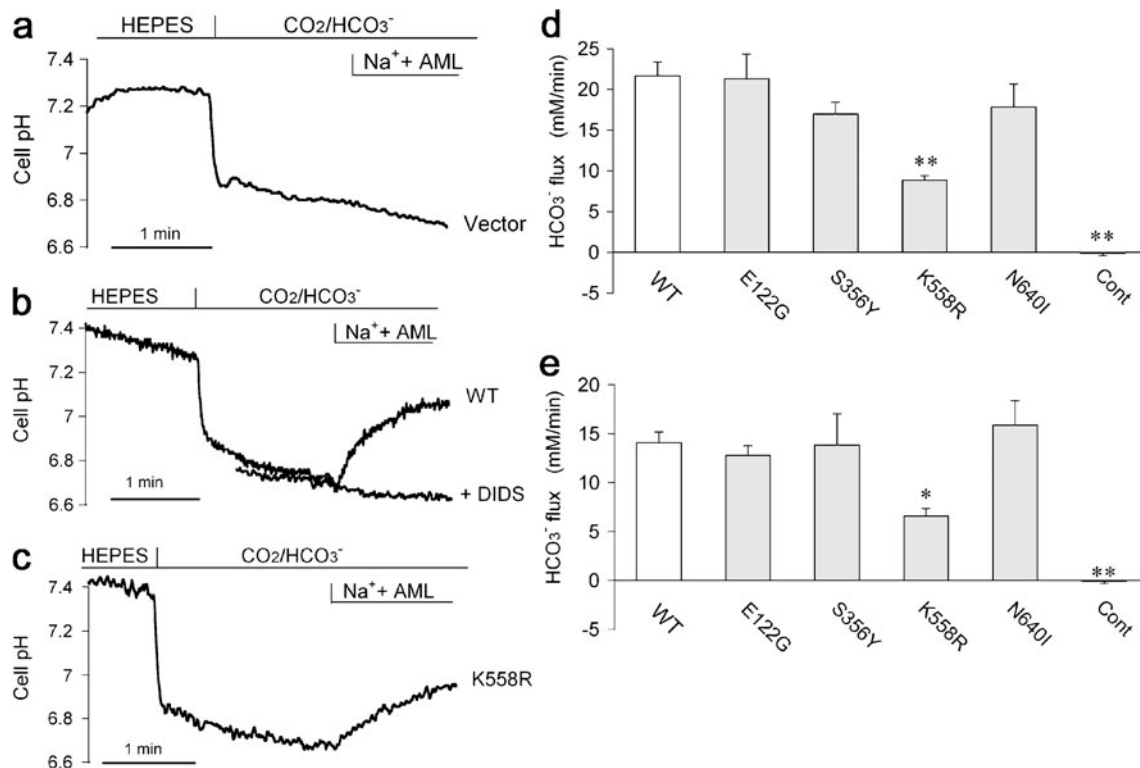


Fig. 6 Functional analysis in HEK293 cells in the presence of HCO₃⁻/CO₂. **a–c** Original traces for cells transfected with vector (**a**), WT (**b**), and K558R (**c**) are shown. Note the absence of cell pH recovery in vector, the prompt cell pH recovery in WT that was completely inhibited by DIDS (0.5 mM), and the lower rate of cell pH recovery in K558R than in WT. *AML* amiloride (1 mM). **d** Summary data for NBCe1-mediated HCO₃⁻ fluxes by the GFP-tagged con-

structs. *Cont* cells transfected vector alone. ***p*<0.01 vs. WT. Numbers of observation are 26 (*WT*), 9 (*E122G*), 9 (*S356Y*), 22 (*K558R*), 21 (*N640I*), and 12 (*Cont*). **e** Summary data for NBCe1-mediated HCO₃⁻ fluxes by the GFP-untagged constructs. **p*<0.05 vs. WT. Numbers of observation are 14 (*WT*), 10 (*E122G*), 7 (*S356Y*), 12 (*K558R*), 11 (*N640I*), and 9 (*Cont*)

wild-type activity. Furthermore, all of the variants had surface expression comparable to that of wild-type NBCe1 in HEK293 cells. From these results, we conclude that while the K558R variant significantly reduces the NBCe1A activity without changing the trafficking behavior, the remaining three SNPs do not change the NBCe1A properties at all.

Consistent with the previous reports [4, 24, 40, 45], our functional analysis in HEK293 cells confirmed the absolute dependence of NBCe1 activity on Na⁺. On the other hand,

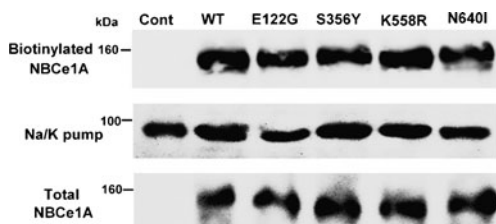


Fig. 7 Cell surface expression of NBCe1A. Blots with the anti-GFP antibody in biotinylated (2 μl per lane) and total fractions (15 μl per lane) are shown. Equal protein loading in biotinylated fractions is confirmed by blots with anti-Na/K pump. A representative blot from three independent experiments is shown

we observed a small transport activity of NBCe1A even in the absence of HCO₃⁻/CO₂, which corresponds to only 11% of the NBCe1A activity in the presence of HCO₃⁻/CO₂. At present, we cannot definitely determine whether this small residual NBCe1A activity in the absence of HCO₃⁻/CO₂ reflects the very low NBCe1A affinity for OH⁻ [4], or the transport of endogenous HCO₃⁻ metabolically produced by the cells [25].

The significant functional reduction by the K558R variant is consistent with the view that most of the missense

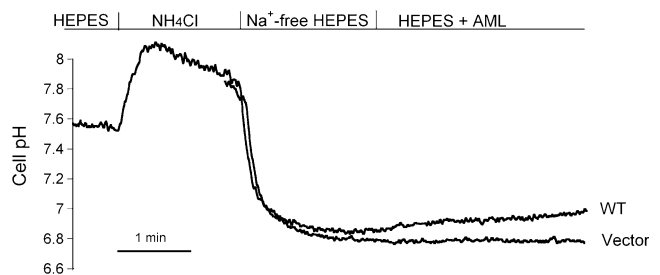


Fig. 8 Functional analysis in HEK293 cells in the absence of HCO₃⁻/CO₂. Cells were acidified by the NH₄Cl (20 mM) pulse. Note that the readdition of Na⁺ induces a slow cell pH recovery in cells transfected with WT. *AML* amiloride (1 mM)

residues causing pRTA lie deep in TMs, where they perform important structural roles [45]. The previous finding that an artificial mutant K558Q had a significantly reduced transport activity corresponding to 53% of that of wild-type [2] further supports the importance of K558. On the other hand, K558, K559, and K562 may constitute the ⁵⁵⁸KKMIK motif, which may represent one of the putative binding sites for DIDS [31]. For example, the ⁵⁵⁸RRMIR mutant had a slightly higher DIDS binding affinity, while ⁵⁵⁸NNMIN mutant had a markedly reduced DIDS binding affinity. However, these mutants had HCO₃⁻ slope conductance comparable to that of wild-type in *Xenopus* oocytes. From these and other results, Lu and Boron [31] concluded that ⁵⁵⁸KKMIK motif is important for the reversible and irreversible interactions with DIDS, but not essential for the electrogenic transport activity of NBCe1A. We speculate that the effect of single amino acid substitution of K558 is different from the simultaneous substitutions of K558, K559 and K562. The significant functional reduction caused by the amino acid substitutions both with (K558Q) or without (K558R) charge alterations rather support a critical role of K558 in the overall NBCe1 transport. It should be mentioned, however, that the amino acid substitutions of NBCe1 by different classes of amino acids would not necessarily induce the similar functional effects. For example, the pRTA-related mutant L522P is predominantly retained in the cytoplasmic region and shows almost no functional activity in mammalian cells [39]. On the other hand, the artificial mutant L522C is properly processed to the plasma membrane and shows a significant activity corresponding to approximately 70% of the wild-type activity in HEK293 cells [45].

Based on the structural similarity in SLC4 bicarbonate transporters and the NBCe1A mutagenesis analysis, Chang et al. [10] previously proposed that E91 is predicted to hydrogen bond with R298, thereby constituting an ion transport pathway together with R86 and E92. Because E122G does not affect the NBCe1A activity, E122 may not be directly involved in this functionally important domain proposed by Chang et al. [10]. The residues near N640 in the extracellular loop have not been extensively analyzed. Only an artificial mutant D647R, predicted to line in the entry of TM6, was shown to markedly reduce the NBCe1 function [2].

Homozygous inactivating mutations in NBCe1 cause pRTA associated with ocular abnormalities and short stature. Functional analyses using the different expression systems have shown that as much as 50% reductions in NBCe1A activity can induce these renal and extra renal phenotypes [13, 14, 16–19, 36, 39]. For example, T485S and G486R do not reach the plasma membrane in *Xenopus* oocytes. However, they show the proper membrane expres-

sion and have reduced transport activities corresponding to approximately 50% of that of wild-type in mammalian cells [16, 39]. These results strongly suggest that the K558R variant, which reduces the NBCe1A activity by at least 50%, should lead to the clinically apparent phenotypes, if present in the homozygous status, though such a pRTA patient has not been found yet. At present, the estimated population frequency of pRTA due to NBCe1 mutations is unknown. However, the severe acidemia found in this disease is expected to impair reproductive fitness. Accordingly, K558R can be subject to purifying selection, which may potentially explain the rare allele frequency (0.014) of this variant.

The situation for the heterozygous status of K558R variant may be different from that for the homozygous status. Haploinsufficiency of NBCe1 in mice is associated with mild acidemia [15]. However, heterozygous human mutations in NBCe1 have not been linked to pRTA, probably due to much higher compensatory ability of renal distal tubules in humans [40]. Nevertheless, 50–60% reduction in NBCe1A activity by the K558R variant should have a substantial effect on the overall sodium handling by the kidney, even in the heterozygous status. Notably, rare heterozygous mutations in renal salt handling genes such as *SCL12A3*, *SLC12A1*, and *KCNJI* have been shown to result in the lower blood pressure [23]. In fact, the mean long-term systolic blood pressure among mutation carriers was found to be 6.3 mmHg lower than the mean of the cohort [23]. In view of the large capacity of proximal tubules to reabsorb sodium, it will be interesting to examine in the future studies whether the heterozygous status of K558R variant is also linked to health benefit through the reduction of blood pressure. On the other hand, Kao et al. [24] recently found that NBCe1, like Cl⁻/HCO₃⁻ exchanger AE1, is predominantly a homodimer that is composed of functionally active monomers. We have recently shown that the heterozygous S982NfsX4 mutation, which retains in the endoplasmic reticulum, causes migraine and normal-tension glaucoma through the hetero-oligomer formation with wild-type NBCe1 [40]. However, the K558R variant is quite unlikely to have such a dominant negative effect, because it shows the normal trafficking behavior in the mammalian cells.

In summary, we performed functional characterization of the four nonsynonymous SNPs, E122G, S356Y, K558R, and N640I in NBCe1A. The results indicate that only the K558R variant inactivates the NBCe1 function without changing the apparent Na⁺ affinity or the membrane trafficking behavior.

Acknowledgment This study was supported in part by grants from the Ministry of Education, Culture, Sports, Science and Technology of Japan.

References

- Abuladze N, Song M, Pushkin A, Newman D, Lee I, Nicholas S, Kurtz I (2000) Structural organization of the human NBC1 gene: kNBC1 is transcribed from an alternative promoter in intron 3. *Gene* 251:109–122
- Abuladze N, Azimov R, Newman D, Sassani P, Liu W, Tatishchev S, Pushkin A, Kurtz I (2005) Critical amino acid residues involved in the electrogenic sodium-bicarbonate cotransporter kNBC1-mediated transport. *J Physiol* 565:717–730
- Alper SL (2002) Genetic diseases of acid-base transporters. *Annu Rev Physiol* 64:899–923
- Amlal H, Wang Z, Burnham C, Soleimani M (1998) Functional characterization of a cloned human kidney $\text{Na}^+:\text{HCO}_3^-$ cotransporter. *J Biol Chem* 273:16810–16815
- Bachmann O, Rossmann H, Berger UV, Colledge WH, Ratcliff R, Evans MJ, Gregor M, Seidler U (2003) cAMP-mediated regulation of murine intestinal/pancreatic $\text{Na}^+/\text{HCO}_3^-$ cotransporter subtype pNBC1. *Am J Physiol Gastrointest Liver Physiol* 284:G37–G45
- Bachmann O, Franke K, Yu H, Riederer B, Li HC, Soleimani M, Manns MP, Seidler U (2008) cAMP-dependent and cholinergic regulation of the electrogenic intestinal/pancreatic $\text{Na}^+/\text{HCO}_3^-$ cotransporter pNBC1 in human embryonic kidney (HEK293) cells. *BMC Cell Biol* 9:70
- Bevensee MO, Schmitt BM, Choi I, Romero MF, Boron WF (2000) An electrogenic $\text{Na}^+-\text{HCO}_3^-$ cotransporter (NBC) with a novel COOH^- terminus, cloned from rat brain. *Am J Physiol Cell Physiol* 278:C1200–C1211
- Bok D, Schibler MJ, Pushkin A, Sassani P, Abuladze N, Naser Z, Kurtz I (2001) Immunolocalization of electrogenic sodium-bicarbonate cotransporters pNBC1 and kNBC1 in the rat eye. *Am J Physiol Ren Physiol* 281:F920–F935
- Brune T, Fetzer S, Backus KH, Deitmer JW (1994) Evidence for electrogenic sodium-bicarbonate cotransport in cultured rat cerebellar astrocytes. *Pflugers Arch* 429:64–71
- Chang MH, DiPiero J, Sonnichsen FD, Romero MF (2008) Entry to "formula tunnel" revealed by SLC4A4 human mutation and structural model. *J Biol Chem* 283:18402–18410
- Chesler M (2003) Regulation and modulation of pH in the brain. *Physiol Rev* 83:1183–1221
- Crowley SD, Gurley SB, Herrera MJ, Ruiz P, Griffiths R, Kumar AP, Kim HS, Smithies O, Le TH, Coffman TM (2006) Angiotensin II causes hypertension and cardiac hypertrophy through its receptors in the kidney. *Proc Natl Acad Sci USA* 103:17985–17990
- Demirci FY, Chang MH, Mah TS, Romero MF, Gorin MB (2006) Proximal renal tubular acidosis and ocular pathology: a novel missense mutation in the gene (SLC4A4) for sodium bicarbonate cotransporter protein (NBCe1). *Mol Vis* 12:324–330
- Dinour D, Chang MH, Satoh J, Smith BL, Angle N, Knecht A, Serban I, Holtzman EJ, Romero MF (2004) A novel missense mutation in the sodium bicarbonate cotransporter (NBCe1/SLC4A4) causes proximal tubular acidosis and glaucoma through ion transport defects. *J Biol Chem* 279:52238–52246
- Gawenis LR, Bradford EM, Prasad V, Lorenz JN, Simpson JE, Clarke LL, Woo AL, Grisham C, Sanford LP, Doetschman T, Miller ML, Shull GE (2007) Colonic anion secretory defects and metabolic acidosis in mice lacking the NBC1 $\text{Na}^+/\text{HCO}_3^-$ cotransporter. *J Biol Chem* 282:9042–9052
- Horita S, Yamada H, Inatomi J, Moriyama N, Sekine T, Igarashi T, Endo Y, Dasouki M, Ekim M, Al-Gazali L, Shimadzu M, Seki G, Fujita T (2005) Functional analysis of NBC1 mutants associated with proximal renal tubular acidosis and ocular abnormalities. *J Am Soc Nephrol* 16:2270–2278
- Igarashi T, Inatomi J, Sekine T, Cha SH, Kanai Y, Kunimi M, Tsukamoto K, Satoh H, Shimadzu M, Tozawa F, Mori T, Shiobara M, Seki G, Endou H (1999) Mutations in SLC4A4 cause permanent isolated proximal renal tubular acidosis with ocular abnormalities. *Nat Genet* 23:264–266
- Igarashi T, Inatomi J, Sekine T, Seki G, Shimadzu M, Tozawa F, Takeshima Y, Takumi T, Takahashi T, Yoshikawa N, Nakamura H, Endou H (2001) Novel nonsense mutation in the $\text{Na}^+/\text{HCO}_3^-$ cotransporter gene (SLC4A4) in a patient with permanent isolated proximal renal tubular acidosis and bilateral glaucoma. *J Am Soc Nephrol* 12:713–718
- Inatomi J, Horita S, Braverman N, Sekine T, Yamada H, Suzuki Y, Kawahara K, Moriyama N, Kudo A, Kawakami H, Shimadzu M, Endou H, Fujita T, Seki G, Igarashi T (2004) Mutational and functional analysis of SLC4A4 in a patient with proximal renal tubular acidosis. *Pflugers Arch* 448:438–444
- Ishiguro H, Steward MC, Lindsay AR, Case RM (1996) Accumulation of intracellular HCO_3^- by $\text{Na}^+-\text{HCO}_3^-$ cotransport in interlobular ducts from guinea-pig pancreas. *J Physiol* 495(Pt 1):169–178
- Ishiguro H, Steward MC, Wilson RW, Case RM (1996) Bicarbonate secretion in interlobular ducts from guinea pig pancreas. *J Physiol* 495(Pt 1):179–191
- Jacob P, Christiani S, Rossmann H, Lamprecht G, Vieillard-Baron D, Muller R, Gregor M, Seidler U (2000) Role of $\text{Na}^+/\text{HCO}_3^-$ cotransporter NBC1, Na^+/H^+ exchanger NHE1, and carbonic anhydrase in rabbit duodenal bicarbonate secretion. *Gastroenterology* 119:406–419
- Ji W, Foo JN, O'Roak BJ, Zhao H, Larson MG, Simon DB, Newton-Cheh C, State MW, Levy D, Lifton RP (2008) Rare independent mutations in renal salt handling genes contribute to blood pressure variation. *Nat Genet* 40:592–599
- Kao L, Sassani P, Azimov R, Pushkin A, Abuladze N, Peti-Peterdi J, Liu W, Newman D, Kurtz I (2008) Oligomeric structure and minimal functional unit of the electrogenic sodium bicarbonate cotransporter NBCe1-A. *J Biol Chem* 283:26782–26794
- Krapf R, Alpern RJ, Rector FC Jr, Berry CA (1987) Basolateral membrane Na/base cotransport is dependent on $\text{CO}_2/\text{HCO}_3^-$ in the proximal convoluted tubule. *J Gen Physiol* 90:833–853
- Kunimi M, Seki G, Hara C, Taniguchi S, Uwatoko S, Goto A, Kimura S, Fujita T (2000) Dopamine inhibits renal $\text{Na}^+:\text{HCO}_3^-$ cotransporter in rabbits and normotensive rats but not in spontaneously hypertensive rats. *Kidney Int* 57:534–543
- Li HC, Worrell RT, Matthews JB, Husseinzadeh H, Neumeier L, Petrovic S, Conforti L, Soleimani M (2004) Identification of a carboxyl-terminal motif essential for the targeting of $\text{Na}^+-\text{HCO}_3^-$ cotransporter NBC1 to the basolateral membrane. *J Biol Chem* 279:43190–43197
- Li HC, Szligeti P, Worrell RT, Matthews JB, Conforti L, Soleimani M (2005) Missense mutations in $\text{Na}^+:\text{HCO}_3^-$ cotransporter NBC1 show abnormal trafficking in polarized kidney cells: a basis of proximal renal tubular acidosis. *Am J Physiol Ren Physiol* 289:F61–F71
- Li Y, Yamada H, Kita Y, Kunimi M, Horita S, Suzuki M, Endo Y, Shimizu T, Seki G, Fujita T (2008) Roles of ERK and cPLA2 in the angiotensin II-mediated biphasic regulation of $\text{Na}^+-\text{HCO}_3^-$ transport. *J Am Soc Nephrol* 19:252–259
- Lin S, Lo Y, Yang S, Seki G (2009) Severe metabolic acidosis causes early lethality in NBC1 W516X. *J Am Soc Nephrol* 20:33A
- Lu J, Boron WF (2007) Reversible and irreversible interactions of DIDS with the human electrogenic $\text{Na}^+/\text{HCO}_3^-$ cotransporter NBCe1-A: role of lysines in the KKMik motif of TM5. *Am J Physiol Cell Physiol* 292:C1787–C1798
- Marino CR, Jeanes V, Boron WF, Schmitt BM (1999) Expression and distribution of the $\text{Na}^+-\text{HCO}_3^-$ cotransporter in human pancreas. *Am J Physiol* 277:G487–G494
- Romero MF, Hediger MA, Boulpaep EL, Boron WF (1997) Expression cloning and characterization of a renal electrogenic $\text{Na}^+/\text{HCO}_3^-$ cotransporter. *Nature* 387:409–413

34. Romero MF, Boron WF (1999) Electrogenic $\text{Na}^+/\text{HCO}_3^-$ cotransporters: cloning and physiology. *Annu Rev Physiol* 61:699–723
35. Roussa E, Nastainczyk W, Thevenod F (2004) Differential expression of electrogenic NBC1 (SLC4A4) variants in rat kidney and pancreas. *Biochem Biophys Res Commun* 314:382–389
36. Satoh H, Moriyama N, Hara C, Yamada H, Horita S, Kunimi M, Tsukamoto K, Iso ON, Inatomi J, Kawakami H, Kudo A, Endou H, Igarashi T, Goto A, Fujita T, Seki G (2003) Localization of $\text{Na}^+/\text{HCO}_3^-$ cotransporter (NBC-1) variants in rat and human pancreas. *Am J Physiol Cell Physiol* 284:C729–C737
37. Schmitt BM, Berger UV, Douglas RM, Bevenssee MO, Hediger MA, Haddad GG, Boron WF (2000) Na/HCO_3 cotransporters in rat brain: expression in glia, neurons, and choroid plexus. *J Neurosci* 20:6839–6848
38. Shirakabe K, Priori G, Yamada H, Ando H, Horita S, Fujita T, Fujimoto I, Mizutani A, Seki G, Mikoshiba K (2006) IRBIT, an inositol 1, 4, 5-trisphosphate receptor-binding protein, specifically binds to and activates pancreas-type $\text{Na}^+/\text{HCO}_3^-$ cotransporter 1 (pNBC1). *Proc Natl Acad Sci USA* 103:9542–9547
39. Suzuki M, Vaisbich MH, Yamada H, Horita S, Li Y, Sekine T, Moriyama N, Igarashi T, Endo Y, Cardoso TP, de Sa LC, Koch VH, Seki G, Fujita T (2008) Functional analysis of a novel missense NBC1 mutation and of other mutations causing proximal renal tubular acidosis. *Pflugers Arch* 455:583–593
40. Suzuki M, Van Paesschen W, Stalmans I, Horita S, Yamada H, Bergmans BA, Legius E, Riant F, De Jonghe P, Li Y, Sekine T, Igarashi T, Fujimoto I, Mikoshiba K, Shimadzu M, Shiohara M, Braverman N, Al-Gazali L, Fujita T, Seki G (2010) Defective membrane expression of the $\text{Na}^+/\text{HCO}_3^-$ cotransporter NBCe1 is associated with familial migraine. *Proc Natl Acad Sci USA* 107:15963–15968
41. Tøye AM, Parker MD, Daly CM, Lu J, Virkki LV, Pelletier MF, Boron WF (2006) The human NBCe1-A mutant R881C, associated with proximal renal tubular acidosis, retains function but is mistargeted in polarized renal epithelia. *Am J Physiol Cell Physiol* 291:C788–C801
42. Usui T, Hara M, Satoh H, Moriyama N, Kagaya H, Amano S, Oshika T, Ishii Y, Ibaraki N, Hara C, Kunimi M, Noiri E, Tsukamoto K, Inatomi J, Kawakami H, Endou H, Igarashi T, Goto A, Fujita T, Araie M, Seki G (2001) Molecular basis of ocular abnormalities associated with proximal renal tubular acidosis. *J Clin Invest* 108:107–115
43. Wang T, Yang CL, Abbiati T, Schultheis PJ, Shull GE, Giebisch G, Aronson PS (1999) Mechanism of proximal tubule bicarbonate absorption in NHE3 null mice. *Am J Physiol* 277: F298–F302
44. Woo AL, Noonan WT, Schultheis PJ, Neumann JC, Manning PA, Lorenz JN, Shull GE (2003) Renal function in NHE3-deficient mice with transgenic rescue of small intestinal absorptive defect. *Am J Physiol Ren Physiol* 284:F1190–F1198
45. Zhu Q, Kao L, Azimov R, Newman D, Liu W, Pushkin A, Abuladze N, Kurtz I (2010) Topological location and structural importance of the NBCe1-A residues mutated in proximal renal tubular acidosis. *J Biol Chem* 285:13416–13426